Meccanica
DOI 10.1007/s11012-014-9987-9

ACOUSTIC AND OTHER FORMS OF ENERGY EMISSIONS

Anisotropic and impulsive neutron emissions from brittle rocks under mechanical load

Andrea Manuello Bertetto · Battista Grosso · Roberto Ricciu · Daniele Rizzu

Received: 13 July 2013 / Accepted: 14 June 2014

Abstract The aim of the present research work is to investigate the emission of neutrons from inert materials subjected to mechanical load. If confirmed, this emission can be seen as a proof of the existence of piezonuclear reactions, i.e. nuclear reactions of fission induced by pressure. This investigation was performed by loading specimens of granite under uniaxial compression till failure and recording the emissions through passive dosimeters. In the present work, the experimental setup was designed and realised, in accordance with what is described in the literature as concerns neutron emissions from inert rock specimens under compressive uniaxial loads. The proper functioning of dosimeters was verified and the experimental functional procedure with radioactive sources was described in the paper. The preliminary experimental activity of the measurement of the background level of neutrons was performed describing the set up allowing it. Finally, the functional tests with radioactive sources, measurement of background values and neutron emission tests during the monoaxial destructive compression tests of the granite specimen were compared and discussed.

Keywords Neutron emission · Mechanical load · Piezonuclear reactions · Brittle fracture · Rock crushing failure

A. Manuello Bertetto (✉) · D. Rizzu
Dipartimento di Ingegneria Meccanica Chimica e dei Materiali, Università degli Studi di Cagliari, Cagliari, Italy
e-mail: andrea.manuello@unica.it

B. Grosso · R. Ricciu
Dipartimento di Ingegneria Civile, Ambientale e Architettura, Università degli Studi di Cagliari, Cagliari, Italy

1 Introduction

In the scientific community studies have been conducted on the different forms of energy emitted during the failure of brittle materials based on acoustic emission signals, or on the detection of the electromagnetic charge.

Since first half of the twentieth century, the mechanical induction of nuclear phenomena has been investigated. In particular, between 1962 and 1984 several experiments on solid radioactive materials with neutron production favoured by pressure were performed [1, 2], based on previous knowledge.

The possibility of causing nuclear reactions by subjecting different materials to mechanical load has been investigated, among others, by Taleyarkhan, who conducted experiments producing "piezonuclear" reactions in gas and liquids with dissolved radioactive substances [3].

As authors' knowledge, the first time the scientific community introduced the term "piezonuclear" dates on year 1986, talking about the use of a diamond-anvil high-pressure cell [4].

Published online: 08 July 2014

Neutron emissions coming from piezonuclear reactions in inert liquids containing iron [5] have been observed.

Carpinteri et al. [6], performed experiments with non-radioactive materials and proposed several reactions.

In the first experiments with non-radioactive materials, solutions of water containing iron salts were subjected to cavitation induced by a sonotrode oscillating with the appropriate frequency [7].

Tests have been conducted on damage produced by the exposure of an iron bar to pressure waves [8].

More recently, piezonuclear neutron emissions from brittle rock specimens in compression have been studied [9–11].

The experiments with solid materials were performed subjecting them to mechanical load of monotonic and cyclic compression. In these experiments, a dose of neutrons was measured. The emissions of neutrons took place in conjunction with specimen failure. These emissions were recorded by passive (bubble detectors) and electronic (He-3 devices) instruments [9, 12].

The existence of these reactions has been theorised in [13, 14] and their occurrence appears to be confirmed by the microchemical analyses shown in [15, 16].

In addition, it seems to emerge an indirect evidence of piezonuclear reactions, based on geochemical and geomechanical considerations [17, 18].

In the present work, the research theme was approached from an experimental point of view, subjecting specimens of granite coming from Sardinia to a monotonic load and measuring the eventual emission through passive dosimeters.

2 Experimental equipment and test

The experimental setup, in accordance with what is described in the literature as concerns neutron emissions from inert rock specimens under compressive uniaxial loads, considers specimens of granite meeting the requirements as in [10]: the material containing iron must be fragile and the volume of the specimen must be above a given threshold.

A cutting machine shown in Fig. 1 was used to prepare the specimens. All specimens were of the same prismatic shape and size, measuring $50 \times 50 \times 150$ in millimetres.

Tests have been carried out on a granite coming from the north east of Sardinia and named Rosa Beta. Its main mineral components are quartz SiO_2, feldspar ($KAlSi_3O_8$) (orthoclase, sanidine and microcline), plagioclase ($(Na,Ca)(Si,Al)_4O_8$) and biotite $K(Mg,Fe^{2+})_3[AlSi_3O_{10}(OH,F)_2$. The rock is isotropic and phaneritic in texture. In Tables 1 and 2 the main mechanical properties and the chemical composition are synthesized respectively.

Since neutrons are electrically neutral particles, to detect them a conversion process is used: a secondary charged particle is produced by an incident neutron interacting with a nucleus. This allows an accurate neutron evaluation by the superheated bubble detection technique. Passive neutron bubble detectors, as in Fig. 2, were used; they are insensitive to electromagnetic noise and have zero gamma sensitivity. The dosimeters (BTI, Ontario, Canada, 1992) [19] are based on superheated bubble detectors and are calibrated at the factory against an Americium-Beryllium source as given in NCRP report 38 [20]. Each bubble detector is a polycarbonate vial where there is an elastic tissue equivalent polymer in which droplets of Freon are dispersed. A droplet vaporizes forming a visible gas bubble; this bubble stays trapped in the gel when a neutron collides; the direct measurement of the equivalent neutron dose comes from the number of bubbles. These detectors are suitable for neutron dose measurements in the energy range of thermal neutrons ($E = 0.025$ eV, BDT type) and fast neutrons ($E > 100$ keV, BD-PND type).

A liquid is said to be superheated when it maintains its liquid state above the boiling temperature. The overheated state is a metastable state from the time that the system is in a state of minimum energy, but not in an absolute minimum. For neutron emission, detecting dosimeters are used with chlorofluorocarbons with a moderate degree of overheating; detectors are typically used with emulsions of CCl_2F_2 (Dichlorodifluoromethane). For the formation of bubbles there are threshold values that depend on the composition of the droplets and the condition of temperature and pressure, as well as the degree of overheating of emulsions; the relation between dose and number of bubbles (sensitivity of the dosimeter) is constant regardless of the neutron dose.

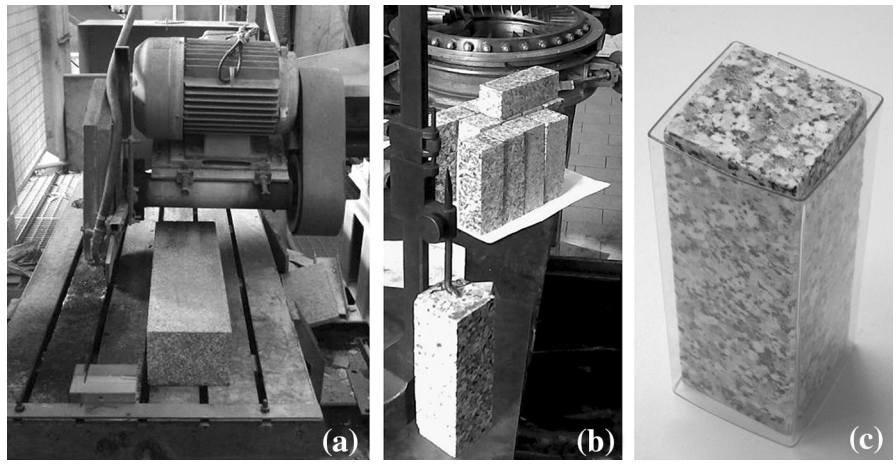

Fig. 1 The cutting diamond disc (**a**), some specimens during the checking of the upper and lower face co-planarity (**b**), a granite specimen (**c**)

Table 1 Mechanical properties of granite

Unit weight	KN/m^3	26.35
Imbibition coefficient	%	0.0035
Thermal linear expansion coefficient	mm/ m °C	7,3 E-6
Compression breaking load	MPa	194.5
Compression breaking load after freeze/ thaw cycles	MPa	169.7
Elasticity modulus	GPa	54
Impact resistance	J	5.01
Frictional wear	mm	2.56
Knoop Micro-hardness	MPa	6.213

Table 2 Chemical composition of granite

SiO_2	71.95 % (silica)
Al_2O_3	14.40 % (alumina)
K_2O	4.12 %
Na_2O	3.68 %
CaO	1.82 %
FeO	1.68 %
Fe_2O_3	1.22 %
MgO	0.71 %
TiO_2	0.30 %
P_2O_5	0.12 %

The dosimeters were initially closed and sealed; they were activated through the removal of the cap, which is equipped with an integrated piston as shown in Fig. 2, that keeps the pressurized liquid contained in the dosimeters. By recompressing the gel through the piston it is possible to return to the initial conditions and the dosimeter can be reused.

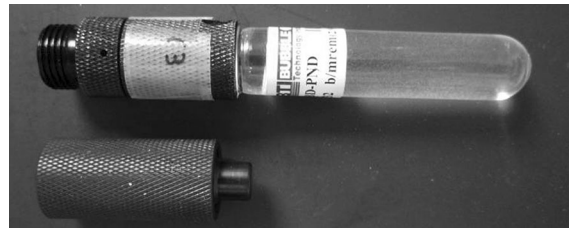

Fig. 2 A dosimeter with its cap

Table 3 Identification of used dosimeters

Tag	Type	Sensitivity		Code
		Bubbles/ mrem	Bubbles/ μSv	
C1	BDT (for thermal neutrons)	32	2.9	11165170
C2	BD-PND (for fast neutrons)	29	2.7	10062234
C3	BD-PND (for fast neutrons)	32	2.9	10062313
C4	BDT (for thermal neutrons)	30	2.7	11249132
C5	BDT (for thermal neutrons)	31	2.8	11165133
C6	BD-PND (for fast neutrons)	32	3.0	10020115

The bubble dosimeters used are indicated by the letters C1,…, C6 as in Table 3, they can be classified as dosimeters for thermal neutrons and for fast neutron measurements.

Fig. 3 The Am–Be source (**a**); tag of Am–Be source (**b**); tag of Cs-137 source (**c**)

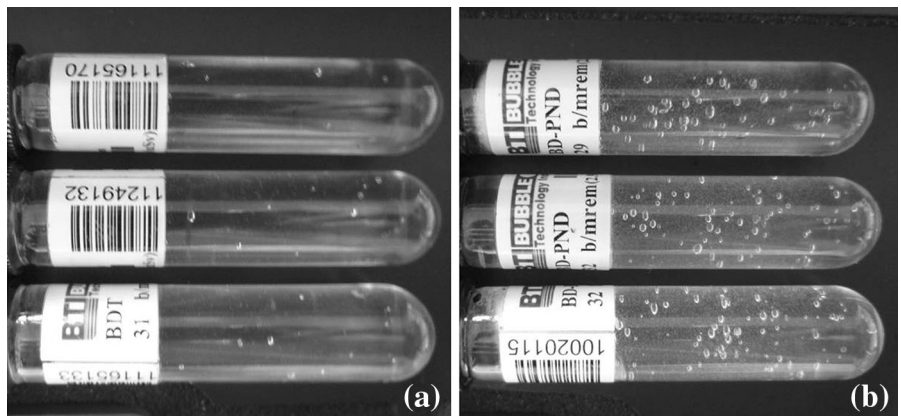

Fig. 4 Dosimeters for slow (**a**) and fast (**b**) neutrons, after the test with radioactive sources

To verify the proper functioning of the dosimeters, they were exposed to two reference radioactive sources. The sources are one of ^{241}Am/Be and one of Cs-137. The sources are placed in a special room with lead-lined walls, inside the Geology Laboratory of the University of Cagliari.

In Fig. 3a the device containing the Am–Be source is shown, while Fig. 3b, c show the labels of the two sources with the indication of activity.

The radioactive elements are enclosed in a steel cylinder. Furthermore, to reduce emissions when not in use, the steel cylinder is surrounded by a polymeric

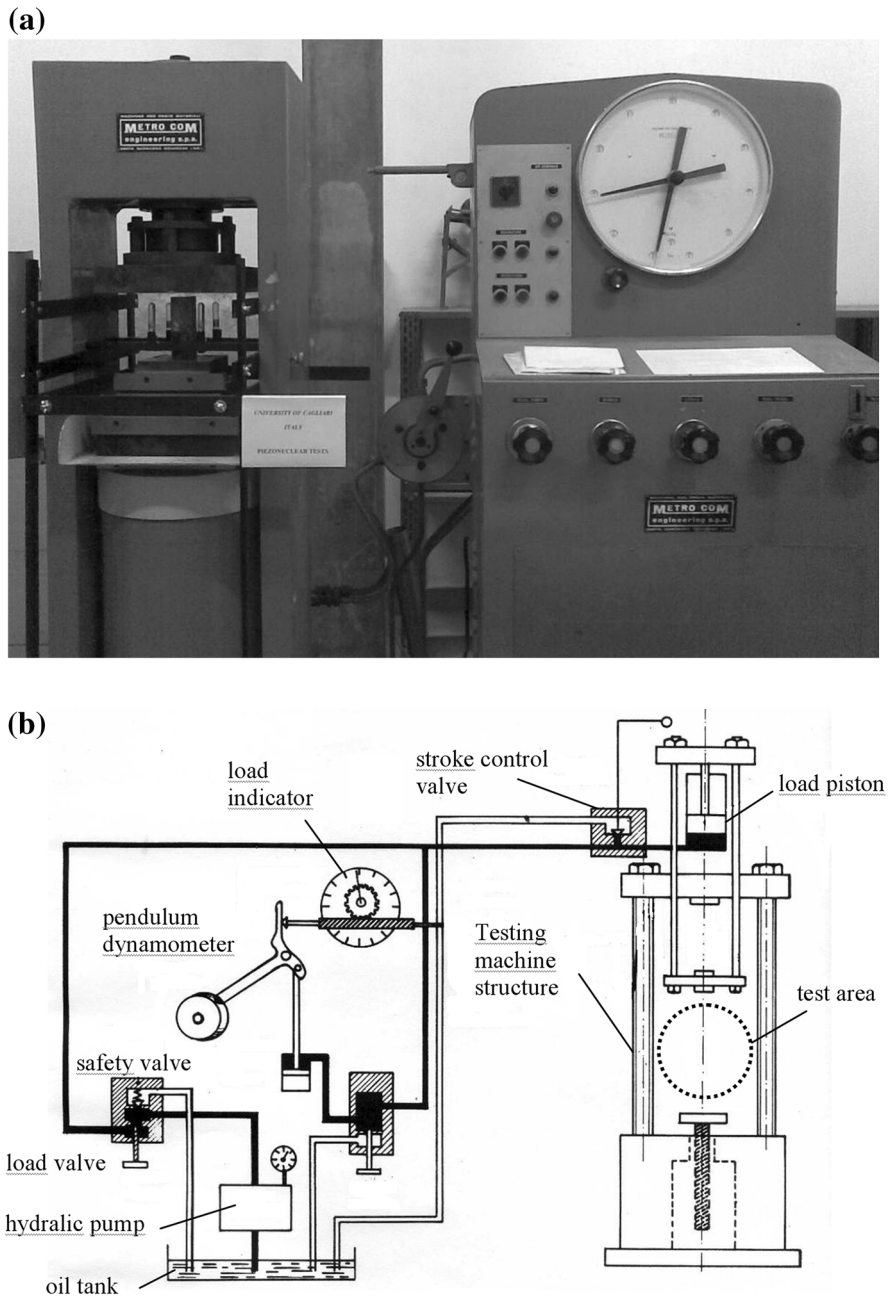

Fig. 5 **a** The testing machine used for compression tests (METRO COM). **b** The diagram of the machine

shield. To perform the test, the steel cylinder is extracted from the shield.

The nominal activity of ^{241}Am/Be source is 0.03 Ci, with half-time of 432 years. Since the experiments have been performed within the recommended working life of the radioactive source, i.e. 15 years, the radioactive activity can be considered equal to its nominal value.

The "fast" dosimeters C2, C3 and C6 showed some bubbles before the test, equal in number, respectively, 4, 2 and 3, but this does not invalidate the test itself. The neutron detectors are moved toward both radioactive sources and checked every 5 min. At the end of the test, which lasted 30 min, the bubbles were counted. At the end of the test the dosimeters for slow neutrons C1, C4 and C5 had 6, 9 and 10 bubbles

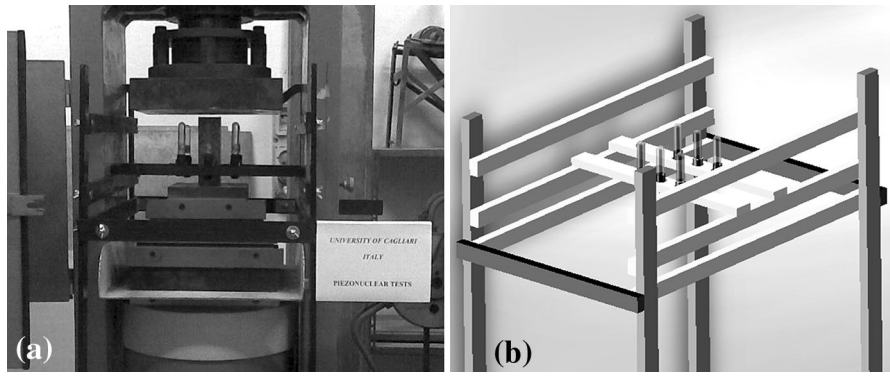

Fig. 6 The in-place dosimeters support

Fig. 7 Layout of shooting and lighting equipment

as shown in Fig. 4a, corresponding to a dose rate of 4.10 ± 0.82, 6.70 ± 1.34 and 7.10 ± 1.42 μSv/h respectively, with an average value of 5.97 ± 1.19 μSv/h. The dosimeters for fast neutrons C2, C3 and C6 showed 56, 69 and 65 bubbles, as shown in Fig. 4b, of which net 52, 67 and 62, corresponding to a dose rate of 38.0 ± 7.6, 46.0 ± 9.2 and 41.0 ± 8.2 μSv/h, with an average value of 42.0 ± 8.4 μSv/h.

To impose the load on the specimens a servo hydraulic testing machine was used. A photograph and a diagram of the machine are shown in Fig. 5. An hydraulic piston moves a plate acting on the specimen. The specimen is pushed against a counterpart plate linked to the frame through a spherical joint, allowing a tolerance in the parallelism between the lower and upper faces of the specimen. The actuator piston moves the plate along a stroke of up to 60 mm. The maximum load is 2.0×10^6 N, to which corresponds an oil pressure of 28 MPa in the hydraulic circuit.

A frame, shown in Fig. 6, was designed and built to hold the dosimeters close to the specimen during tests. It is independent and not connected to the body of the testing machine to avoid being influenced by movements and vibrations. The material of the frame is insensitive to electromagnetic fields. The frame occupies an area around the specimen under test and it is

Fig. 8 The dosimeter frame diagram and the radiometer used to detect the background level in the test room

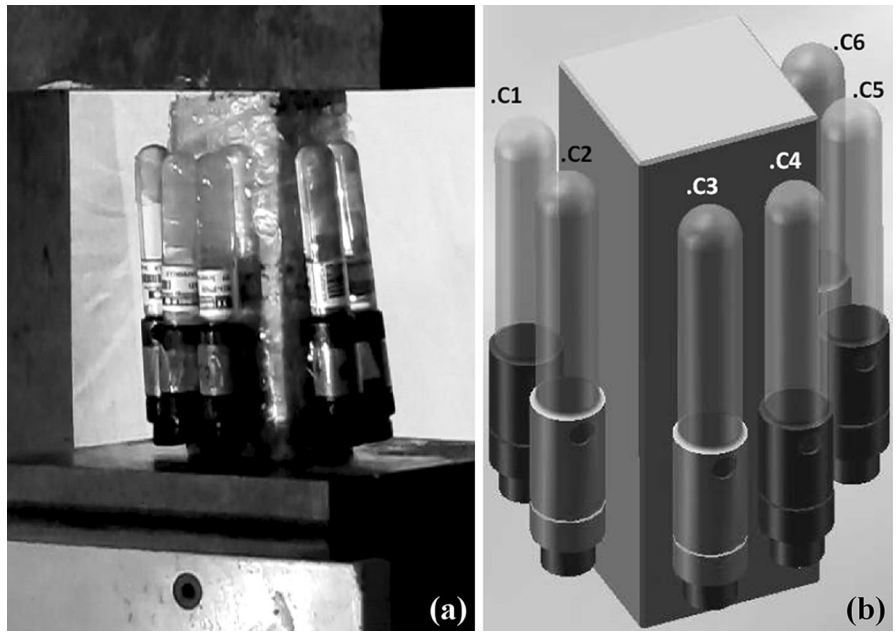

Fig. 9 The dosimeters on the specimen in the test machine and their positioning diagram (see also Table 2)

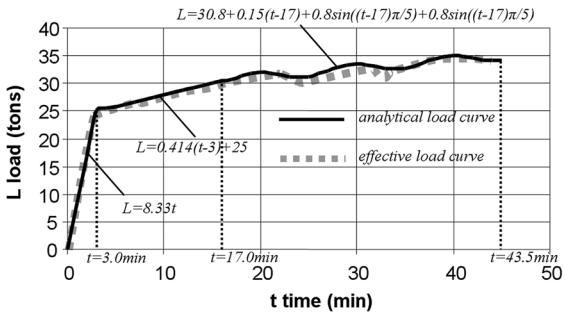

Fig. 10 The load increasing curve versus time in the test no. 3

able to accommodate many dosimeters in different positions, depending on the test requirements.

The dosimeters are positioned on two adjustable horizontal beams supported by the frame. The beams are equipped with different supports which allow different positions of the dosimeters along the beams.

In Fig. 7 the entire test rig is shown. For shooting video a Casio Model EX-F1 digital camera was used. The lighting, in addition to the one typical of the laboratory, was provided by a halogen lamp having a power of 450 W and a flux of 8,000 lumen. A view of the general layout is shown in Fig. 7.

The experimental loading tests were carried out in the University of Cagliari Laboratory of the Civil Engineering, Environment and Architecture Department and in the Laboratory of Applied Mechanics of Mechanical, Chemical and Materials Engineering Department.

Fig. 11 Specimen and dosimeters at the end of test no. 3

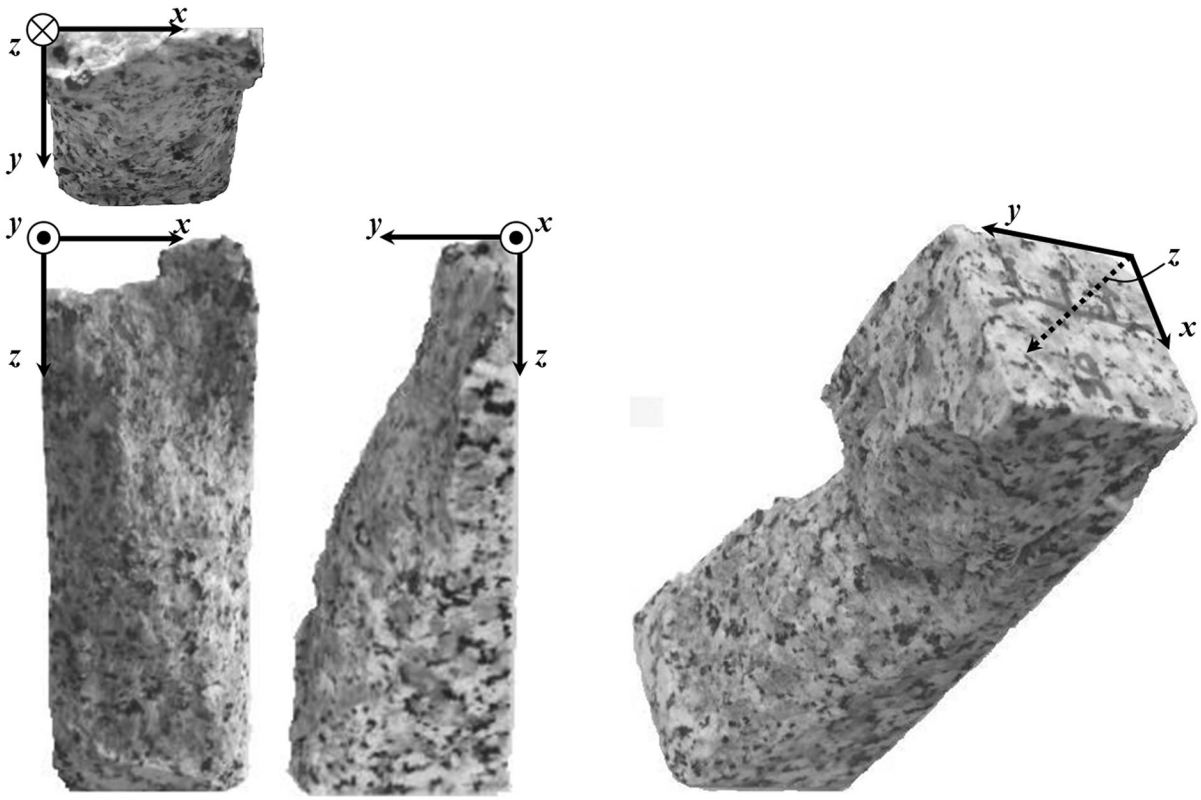

Fig. 12 The collapsed specimen after test no. 3

The test room is a closed underground room. One of the preliminary experimental activities was the measurement of the background level of neutrons. To perform this measurement, the six dosimeters were left in the laboratory for 6 h, mounted on the frame (see Fig. 6b) as in the diagram of Fig. 8a, specially built to assemble them, as previously described, and placed at the centre of the test room. The test duration to determine the background can range between few hours and few days.

In particular, the time required to measure the natural neutron background is about ten hours, as reported in [21].

After that, five of them (C1… C5) showed a bubble each. This corresponds to a dose of 0.345 ± 0.172, $0.370 \pm 0.185, 0.345 \pm 0.172, 0.370 \pm 0.185, 0.357 \pm 0.178$ μSv, respectively, with an average value of 0.362 ± 0.181 μSv, coming from slow neutrons, and 0.364 ± 0.182 μSv, coming from "fast" neutrons. To these doses correspond dose rates of 60.3 ± 30.1 and 60.7 ± 30.3 nSv/h, respectively. These values are of the same order of magnitude as the ones recorded by a radiometer 98.3 ± 0.1 nSv/h as shown in Fig. 8b.

For the measurements performed on the testing machine, the specimens were placed between the plates and the dosimeters were positioned as close to the specimen as possible. The specimens were wrapped in a bubble wrap sheet to prevent damage to instruments and people, following the dispersion of splinters and fragments from the sudden collapse of the specimen being tested.

In Fig. 9a the specimen is represented as positioned in the testing machine before the compression test. The dosimeter distribution around the specimen is shown in the diagram in Fig. 9b. The dosimeters indicated with C1, C4 and C5 are BDT (for thermal neutrons) and C2, C3 and C6 are BD-PND (for fast neutrons).

Eight tests were performed, all of which applying a fast rate of load up to a load of 25 tons and then applying an increasing load having a rate of growth lower than in the first part of the test.

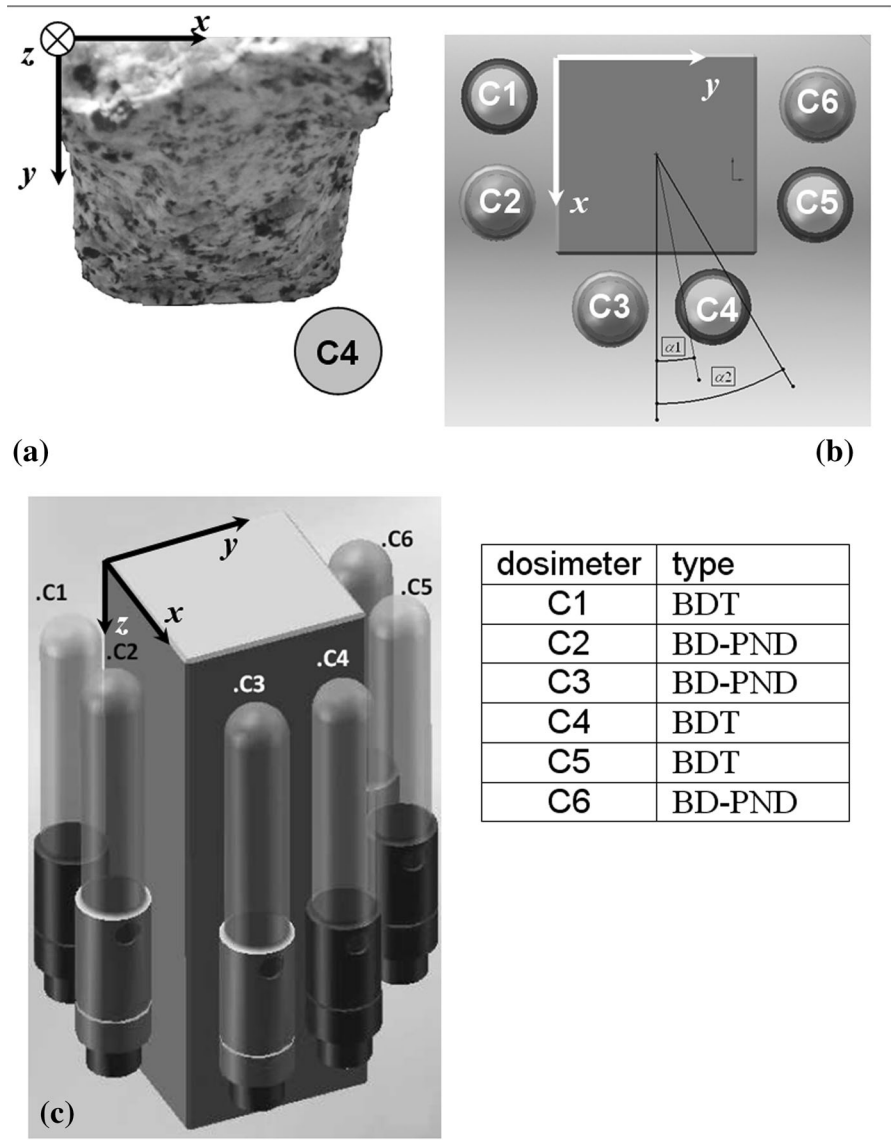

dosimeter	type
C1	BDT
C2	BD-PND
C3	BD-PND
C4	BDT
C5	BDT
C6	BD-PND

Fig. 13 Plan view of the specimen (**a**), plan view diagram (**b**) and axonometric diagram of the dosimeter positioning near the specimen (**c**)

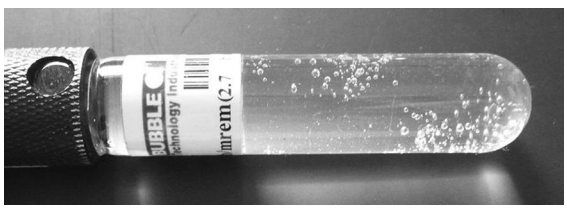

Fig. 14 The C4 dosimeter for thermal neutrons

Test no. 3 gave a particularly significant output. This experiment was performed with the intention of quickly reaching a given load and then keeping the pressure on the sample oscillating around a value so as to trigger the first cracks.

The load curve is drawn in the graph of Fig. 10. The entire curve can be modelled using a load function versus time as a set of three functions on three different time intervals. The three functions are two linear and one sinusoidal. Indicating the test time t in minutes and the load L in tons, for t between 0 and 3 min the load expression could be given by $L = 8.33\,t$; for t between 3 and 17 min the load expression could be given by $L = 0.414\ (t-3) + 25$; for t between 17 and 43.5 min, the load expression could be given by $L = 30.8 + 0.15\ (t-17) + 0.8 \sin((t-17)\pi/5)$.

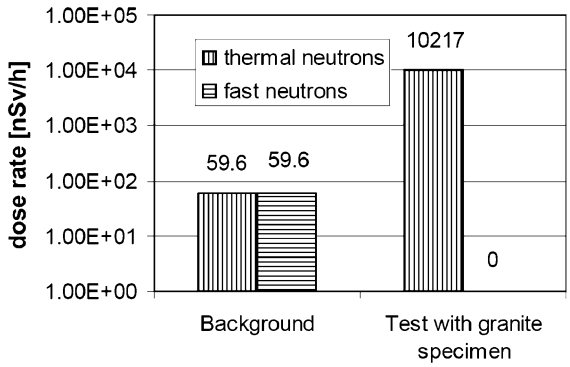

Fig. 15 The different dose rates for fast and thermal dosimeters in two different tests: measurement of background values; neutron emission tests during the monoaxial destructive compression tests of the granite specimen

The collapse occurred 40 min after the start of the test for a load of 35.4 tons, equivalent to a fluid pressure of 139 MPa in the hydraulic circuit. The specimen and dosimeters at the end of test no. 3 are shown in Fig. 11.

In Fig. 12 the photograph on the left hand side shows the specimen after collapse in three orthogonal projections and the recomposed specimen on the right in axonometric view.

In Fig. 13 it is possible to show the dosimeter positioning also schematised in Fig. 9b. In Fig. 13a the photograph represents in plan view the lower part of the collapsed specimen. In Fig. 13b the scheme shows in plan view the specimen with the dosimeters; the direction of the neutron flux ranges between $\alpha 1$ and $\alpha 2$ angles. In Fig. 13c an axonometric scheme of the instrumented specimen can be seen with a table of the dosimeter on the right hand side.

In dosimeter C4, 185 ± 10 bubbles in the cylindrical part were counted. As specified in the manufacturer's data sheet the bubbles in the hemispherical area must be ignored. Dosimeter C4, after test no. 3, is shown in Fig. 14. Most of the counted bubbled, however, are joined in two clusters, and so possibly linked to a false signal. Excluding the two clusters, is it possible to count about 20 bubbles. The 20 bubbles indicate a dose of (7.41 ± 1.48) μSv. To this dose corresponds a dose rate of 10.20 ± 2.04 μSv/h. This refers to a conventional time interval equal to the entire duration of the test, which was 43.5 min. The number of bubbles counted is related to a neutron flow rate of 150 times the background level measured by the C4 dosimeter $(60.5 \pm 30.3$ nSv/h).

In the graph of Fig. 15 the dose rate is referred, in nSv/h, of thermal and fast neutrons, drawn using a logarithmic scale. In the graph two couples of histograms are presented. Each couple shows the values of thermal and fast neutron emission for two different tests. The first couple, on the left, represents the background fluxes detected by dosimeters for fast and thermal neutrons respectively; it can be seen that the values in this couple are very close. The second

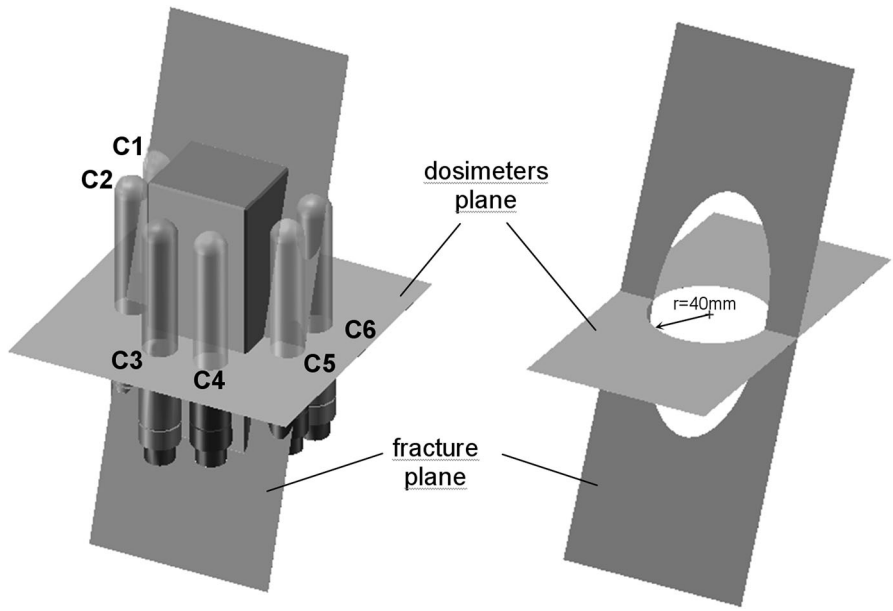

Fig. 16 Dosimeters, specimens and their related planes

couple concerns the destructive test performed on the granite specimen. In this case the dosimeter for fast neutrons shows no output.

Figure 16 shows a diagram of the specimen with two planes describing the test geometry. The two planes are the fracture plane and the dosimeter plane where the base of the sensitive part of the specimens is located. The two planes intersect along a line positioned at mid-height and at mid-thickness of the specimen. The angle between the planes is about 63°. The dosimeters are positioned as in Fig. 9 and it is possible to trace a circumference, having a radius of 40 mm, containing the axis of the dosimeters as in Fig. 15 on the dosimeter plane. The dosimeter that detected a neutron flux was the C4 as mentioned previously.

3 Conclusion

Neutron emission measurements were performed on granite specimens from Sardinia during mechanical compression tests. The authors believe that the presence of piezonuclear reactions giving rise to neutron emissions in inert non-radioactive brittle solids when compression loads are performed on specimens having an opportune size can be assumed. The bubble dosimeters used show neutron fluxes of several orders of magnitude higher than the background level at the time of catastrophic failure. These values correspond to a dose rate of neutrons 150 times the background level measured in the preliminary phase of the test.

The results described in this work and the vitality of the scientific community on this topic encourages exploration of new and fascinating application fields, such as the production of clean nuclear energy and neutrons for medical use in cancer therapy.

Acknowledgments The research reported herein has not been financially supported by any specific grant or agency. However, the authors will acknowledge any form of support for future works on this topic.

References

1. Diebner K (1962) Fusionsprozesse mit Hilfe konvergenter Stoßwellen einige ältere und neuere Versuche und Überlegungen. Kerntechnik 3:89–93
2. Winterberg F (1984) Autocatalytic fusion–fission implosions. Atomenergie-Kerntechnik 44:146
3. Taleyarkhan RP, West CD, Cho JS, Lahey RT Jr, Nigmatulin RI, Block RC (2002) Evidence for nuclear emissions during acoustic cavitation. Science 295:1868–1873. doi:10.1126/science.1067589
4. Van Siclen CDeW, Jones SE (1986) Piezonuclear fusion in isotopic hydrogen molecules. J Phys G Nucl Phys 12:213. doi:10.1088/0305-4616/12/3/009
5. Cardone F, Cherubini G, Petrucci A (2009) Piezonuclear Neutrons. Phys Lett A 373:862–866. doi:10.1016/j.physleta.2008.12.060
6. Carpinteri A, Cardone F, Lacidogna G (2010) Energy emissions from failure phenomena: mechanical, electromagnetic, nuclear. Exp Mech 50:1235–1243. doi:10.1107/s11340-009-9325-7
7. Cardone F, Cherubini G, Magnani R, Perconti W, Petrucci A, Rosetto F, Spera G (2009) Neutrons from piezonuclear reactions. http://aflb.ensmp.fr/AFLB-342/aflb342m669.pdf. Accessed 5 July 2013
8. Albertini G, Calbucci V, Cardone F, Petrucci A, Ridolfi F (2014) Chemical changes induced by ultrasound in iron. Appl Phys A 114:1233–1246. doi:10.1007/s00339-013-7876-z
9. Carpinteri A, Cardone F, Lacidogna G (2009) Piezonuclear neutrons from brittle fracture: early results of mechanical compression tests. Strain 45:332–339. doi:10.1111/j.1475-1305.2008.00615.x
10. Carpinteri A, Borla O, Lacidogna G, Manuello A (2010) Neutron emissions in brittle rocks during compression tests: monotonic vs. cyclic loading. Phys Mesomech 13(5):268–274. doi:10.1016/j.physme.2010.11.007
11. Cardone F, Mignani R, Petrucci A (2012) Piezonuclear reactions. J Adv Phys 1:3–36. doi:10.1166/jap.2012.1015
12. Cardone F, Carpinteri A, Lacidogna G (2009) Piezonuclear neutrons from fracturing of inert solids. Phys Lett A 373:4158–4163. doi:10.1016/j.physleta.2009.09.026
13. Cardone F, Mignani R (2007) Deformed spacetime. Springer, Dordrecht
14. Mignani R, Cardone F, Petrucci A (2014) Generalized lagrange structure of deformed minkowski spacetime. Natural Sci 6:399–410. doi:10.4236/ns.2014.66040
15. Carpinteri A, Chiodoni A, Manuello A, Sandrone R (2011) Energy dispersive X-ray spectroscopy analysis on rock samples subjected to piezonuclear tests. In: Conference proceedings of the society for experimental mechanics, pp 49–56
16. Carpinteri A, Lacidogna G, Manuello A, Borla O (2010) Piezonuclear transmutations in brittle rocks under mechanical loading: microchemical analysis and geological confirmations. Recent Adv Mech 361–382. doi:10.1007/978-94-007-0557-9_19
17. Carpinteri A, Manuello A (2012) An indirect evidence of piezonuclear fission reactions: geomechanical and geochemical evolution in the Earth's crust. Phys Mesomech 15:14–23
18. Carpinteri A, Manuello A (2011) Geomechanical and geochemical evidence of piezonuclear fission reactions in the earth's crust. Strain 47(s2):267–281. doi:10.1111/j.1475-1305.2010.00766.x
19. Bubble Technology Industries (1992) Bubble detector datasheet. http://www.bubbletech.ca/pdfs/BTI_BUBBLE_General_May72009.pdf. Accessed 5 July 2013

20. National Council on Radiation Protection and Measurements Protection Against Neutron Radiation (1971) NCRP Report No. 038
21. Korun M, Martinčič R, Pucelj B (1996) Neutron Measurement by in situ Gamma-ray spectrometry using cadmium converters. J. Stefan Institute, Ljubjiana, Slovenia. http://www.irpa.net/irpa9/cdrom/VOL.2/V2_171.PDF. Accessed 14 April 2014